

# Structural optimization and spiralling of the grain in a pine trunk

Andrej Cherkaev and Seubpong Leelavanichkul

*Department of Mathematics, University of Utah, Salt Lake City, UT 84112 USA*

---

## 1 Introduction

### 1.1 *The phenomenon*

**1.1.0.1 Evolution and optimization criteria** We observe that some trees have grains spiralling around their trunk. An example is Ponderosa pine that grows in rocky windy terrains in South West of the United State (Utah, Anizona, Nevada). One wonders what an evolution significance of such design is. The paper concerns with morphology of tree's trunk from structural optimization viewpoint. Specifically, we investigate the reasons behind spiral grows of the Ponderosa pine trunk in southern Utah. These trees develop helioidal wood fibers that wiggle around the trunk. Spiral grains can be seen on many trees when their barks are removed from the trunks. The spiralling angle is about  $30^\circ - 50^\circ$ . The question is why they twist. The considered problem is an example of the inverse optimization problem [5] that arrives in evolution biology.

Studying morphology like bones or trees' trunks that are critical for the survival of the species, we may postulate that they are optimally adapted to the environment. Trees' trunks should stay unbroken and be able to sustain extreme wind loads applied from all directions. If a natural design becomes more complex, there must be a good reason for this. We treat the evolutionary development of the species as the minimizing sequence of an optimization problem with unknown objective. Many different reasons and hypotheses have been suggested to explain the spiralling, among them are such exotic factors as the earth rotation, the wind, and even the gravitational effect of the moon [7].

**1.1.0.2 Factors that control the spiralling of the grains** Here, we attempt to find the answer considering the morphology of a trunk as a result

of an optimization of a mechanical construction. We model the trunk as an anisotropic cylinder with helicoidal symmetry, compute the stresses, and optimize the angle of the grains inclination using a failure criterion. When the structure of the tree is optimized only for the strength, the objective remains practically neutral to the variation of the angle of spiralling if the angle does not exceed a limit, then the strength declines. The measured angle on the Ponderosa pine in Southern Utah corresponds to this limit. Additional mechanical features of twisted trunks are discussed in Section 4

Why does the tree develop the maximally possible (from the strength perspective) angle of spiralling? We assume, that another biological factor must be considered: The transportation of the fluid from the roots to the branches. The theory worked out by Kubler [8] provides a convincing qualitative reason for the spiralling. The tree's branches with straight grain are fed only by those roots directly below them. Each grain transports the water from the root to the branch above it. These trees grow in the rocky terrains where often half of the roots on one side of the tree meets a solid rock. These roots are reduced and they do not supply water to the corresponding branches. The spiralling allows the uniform watering of the branches across the trunk even if the roots grow from one side only. If all the roots on one side die, that side of the tree is still healthy. This has been proven [8] by injecting conifers with dye at the base. In addition to this consideration, trees become less stiff and bend more easily because of the spiralling grain. The bending allows trees to become more effective at discarding excessive snow from their branches and more resistant to breakage from heavy wind.

**1.1.0.3 About inverse optimization problems** Notice that the optimization problems in engineering and in biology are mutually reciprocal. The biological structure is known, but it is not clear in what sense the structure is optimal. By contrast, the goal of the engineering is the minimization of a given functional that is not the subject of a search; the problem is to find an unknown optimal structure. This observation reflects the principal difference between biology that seeks an answer to the question: Why are the bio-materials and the biomimetics of living organisms the way they are and how to make an optimal structure.

## 1.2 Optimization problem

This qualitative analysis, however, does not tell us how large the angle of the spiralling is. This paper performs stress analysis to estimate that angle. Based on the above consideration, we claim that the design of the trunk corresponds to a solution to the following problem of structural optimization:

Given a axisymmetric cylinder (the trunk) from an orthotropic elastic material (the wood), find the variable angle of inclination of the main axes of anisotropy to the cylinder's axes, which reduces its strength to the value less than a certain level.

The structure of the paper is as follows. In the next section, we analyze the stresses in an anisotropic cylinder that models the tree's trunk. This stress analysis considers the structure under an axial loading and bending moment. The stresses are computed as a function of the grain angle. The analysis of the stresses in the anisotropic cylinder with helicoidal symmetry under bending and compression loads is performed by introducing elastic potentials which generalize the potentials for cylindrical anisotropy.

The objective is to determine the influence of the grain angle on the strength of the structure. To estimate the strength, the Tsai-Hill failure criterion is used. We demonstrate that our numerical results are in agreement with the observed values of the angle of grain spiralling. Additional factors are considered in Sec 4

## 2 Analysis

### 2.1 Linear stress analysis

The displacements are solved directly from the divergence of stress without the presence of the body forces.

$$\nabla \cdot \boldsymbol{\sigma} = 0 \tag{1}$$

We consider the general case of the elastic equilibrium of a loaded homogeneous cylinder having cylindrical anisotropy. The problem is such that at each point, there are no planes of elastic symmetry normal to the generators, and therefore, the cross sections do not remain plane after deformation. We approach this problem by solving the equilibrium equations for the displacement. The objective of this part is to obtain the stress field and the displacement functions for a structure with cylindrically anisotropy.

#### 2.1.1 Generalized plane strain

We analyze the structure with a helicoidal anisotropy, which possesses 13 elastic constants. Its stress-strain relationship in the cylindrical coordinate can be expressed as following [4]:

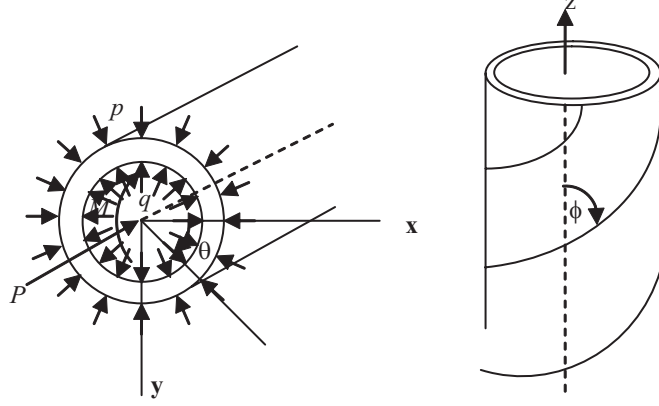


Fig. 1. Schematic of the cylindrical anisotropic body under various loads.

$$\begin{Bmatrix} \varepsilon_{rr} \\ \varepsilon_{\theta\theta} \\ \varepsilon_{zz} \\ \varepsilon_{\theta z} \\ \varepsilon_{rz} \\ \varepsilon_{r\theta} \end{Bmatrix} = \begin{bmatrix} c_{11} & c_{12} & c_{13} & c_{14} & 0 & 0 \\ c_{12} & c_{22} & c_{23} & c_{24} & 0 & 0 \\ c_{13} & c_{23} & c_{33} & c_{34} & 0 & 0 \\ c_{14} & c_{24} & c_{34} & c_{44} & 0 & 0 \\ 0 & 0 & 0 & 0 & c_{55} & c_{56} \\ 0 & 0 & 0 & 0 & c_{56} & c_{66} \end{bmatrix} \begin{Bmatrix} \sigma_{rr} \\ \sigma_{\theta\theta} \\ \sigma_{zz} \\ \sigma_{\theta z} \\ \sigma_{rz} \\ \sigma_{r\theta} \end{Bmatrix} \quad (2)$$

The compliance matrix is obtained by rotating matrix [10] from the material local coordinate to the cylindrical coordinate. For such structure (Fig 1), there exists no antiplane nor plane strain; all three displacements are coupled and depend only on  $r$  and  $\theta$ . The strain  $\varepsilon_{zz}$  is not zero because the structure has a finite length and a finite region of the cross section.

The approximated solutions for displacements of the generalized plane strain are given as follow [9]

$$u = U(r, \theta) - \frac{z^2}{2} (A \cos \theta + B \sin \theta) + u_1 \quad (3)$$

$$v = V(r, \theta) - \frac{z^2}{2} (B \cos \theta - A \sin \theta) + v_1 + \vartheta rz \quad (4)$$

$$w = W(r, \theta) - z (Ar \cos \theta + Br \sin \theta + C) + w_1 \quad (5)$$

where  $u_1$ ,  $v_1$ , and  $w_1$  represent rigid-body displacements.  $A$ ,  $B$ ,  $C$ , and  $\vartheta$  are constants that can be determined from the boundary conditions. Relating the displacements to stresses in (2) via strain-displacement relation and solving (1), the displacement functions are obtained.

### 2.1.2 Displacement functions

Two load cases are considered, axial load and pure bending. Assuming small deformations, these cases are solved separately and combined for total stress afterward. The solutions to the equilibrium equations are sought in the form of power series. Neglecting rigid-body displacements, the displacements are found as follow:

- **Case 1:** Axial loading with external and internal pressure:

$$U(r, \theta) = (U_1 r + U_2 r^{a_1} + U_3 r^{-a_1} + U_p r) \quad (6)$$

$$V(r, \theta) = W(r, \theta) = 0 \quad (7)$$

- **Case 2:** Pure bending with external and internal pressure:

$$U(r, \theta) = (U_0 r^{a_0} + U_1 r^{a_1} + U_2 r^{-a_1} + U_3 r^{a_2} + U_4 r^{-a_2} + U_p r^2) \sin \theta \quad (8)$$

$$V(r, \theta) = (V_0 r^{a_0} + V_1 r^{a_1} + V_2 r^{-a_1} + V_3 r^{a_2} + V_4 r^{-a_2} + V_p r^2) \cos \theta \quad (9)$$

$$W(r, \theta) = (W_0 r + W_1 r^{a_1} + W_2 r^{-a_1} + W_3 r^{a_2} + W_4 r^{-a_2} + W_p r^2) \cos \theta \quad (10)$$

The unknown constants,  $U_i$ ,  $V_i$ , and  $W_i$  ( $i = 0..4$ ) are determined from the boundary conditions. The subscript  $p$  denotes the particular solution.

### 2.2 Nonlinear stress analysis

The linear analysis is applicable when the deformation is small in comparison to the geometry of the structure. However, when the transverse deflection is large, extra moment is generated by the axial load and the problem becomes nonlinear.

The finite element method (FEM) is used in the nonlinear analysis. A 3-D eight node element as shown in Fig 2 is used for the computation. The element has three degree of freedoms,  $u_x$ ,  $u_y$ , and  $u_z$ . The shape functions are obtained from the following displacement functions [1]:

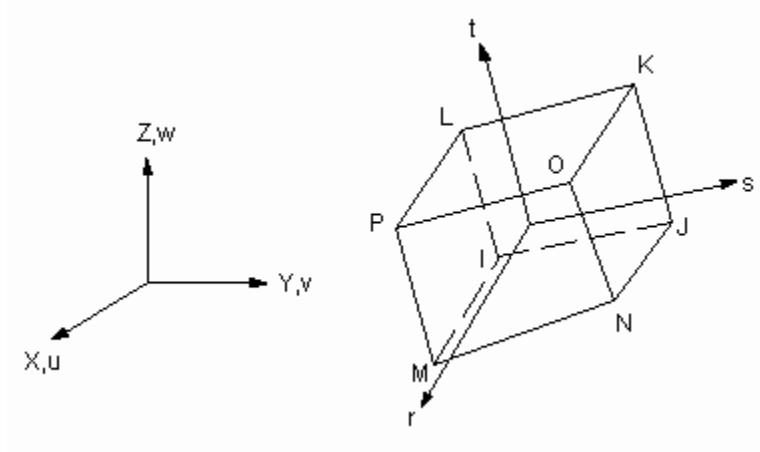


Fig. 2. Sketch of element and its coordinates.

$$\begin{aligned}
 u &= \frac{1}{8} [u_I(1-s)(1-t)(1-r) + u_J(1+s)(1-t)(1-r) \\
 &\quad + u_K(1+s)(1+t)(1-r) + u_L(1-s)(1+t)(1-r) \\
 &\quad + u_M(1-s)(1-t)(1+r) + u_N(1+s)(1-t)(1+r) \\
 &\quad + u_O(1+s)(1+t)(1+r) + u_P(1-s)(1+t)(1+r) \\
 &\quad + u_M(1-s)(1-t)(1+r) + u_N(1+s)(1-t)(1+r)] \\
 &\quad + u_1(1-s^2) + u_2(1-t^2) + u_3(1-r^2) \\
 v &= \frac{1}{8} [v_I(1-s) \text{ an analogous to } u \\
 w &= \frac{1}{8} [w_I(1-s) \text{ an analogous to } u
 \end{aligned}$$

The tree is model as a cylinder having constraints in all degree of freedoms at one end while a surface pressure equivalent to the axial load is applied normal to the cross-section at the other end. A moment is generated at the free end by the applied couple.

### 2.3 Failure criteria

Due to the nature of the anisotropy, the conventional maximum strength criterion for isotropic materials gives a poor prediction of failure. Instead, Tsai-Hill failure criterion is used to predict the failure of a structure that have an anisotropic body.

$$\left( \frac{\sigma_1}{\sigma_{1u}} \right)^2 + \left( \frac{\sigma_2}{\sigma_{2u}} \right)^2 - \frac{\sigma_1 \sigma_2}{\sigma_{1u}^2} + \left( \frac{\tau_{12}}{\tau_{12u}} \right)^2 < 1 \quad (11)$$

Subscripts 1, 2, and 12 indicates the fiber and the transverse direction. The

Table 1  
Elastic moduli of Ponderosa pine with 12 % moisture content, GPa.

$E_1$	$E_2$	$E_3$	$G_{12}$	$G_{13}$	$G_{23}$	$\nu_{31}$	$\nu_{32}$	$\nu_{12}$	$\nu_{21}$	$\nu_{13}$	$\nu_{23}$
0.85	0.51	10.1	0.065	0.71	0.67	0.337	0.4	0.426	0.359	0.41	0.033

subscript  $u$  denotes the ultimate strength of the material in that corresponding direction. When the left hand side of (11) is greater than or equal to 1, the failure is predicted. No distinction is made between compressive and tensile stresses.

### 3 Analysis of Ponderosa pine

#### 3.1 Setting of the parameters

The trunk of the Ponderosa pine is assumed to be a cylinder having radius  $r = 0.254$  m. The axial load has the magnitude  $P = 22$  kN. The bending moment is 57 kN·m. The material properties of the Ponderosa pine are shown in Table 1 [3]. Material strengths are [6]:  $\sigma_{33t} = 43$  MPa,  $\sigma_{33c} = -36$  MPa,  $\sigma_{22t} = 2.8$  MPa,  $\sigma_{22c} = -5.1$  MPa,  $\tau_{23ul} = 8$  MPa.

#### 3.2 Strength of the Ponderosa pine and its failure prediction

The results are shown in the form of failure prediction as a function of spiralling angle (Fig 3 and 4). The + and - in the legends represent  $\theta = \pi/2$  and  $\theta = -\pi/2$ .

The results from Fig 3 and 4 show that the failure prediction value increases slowly to about  $30^\circ$ , and then the slope increases dramatically beyond this point. The tree strength is not sacrificed considerably, as long as the grain angle remains below  $30^\circ$ . Moreover, the failure predictions from both plots yield the similar result only up to this angle. The nonlinear analysis shows that the structure is most likely to fail when the grain angle is  $60^\circ$ . In contrast, the linear analysis indicates  $90^\circ$  for the same geometry and loading parameters. As the wind force causes the tree to bend, the axial loading due to leaves and snow generate the bending moment.

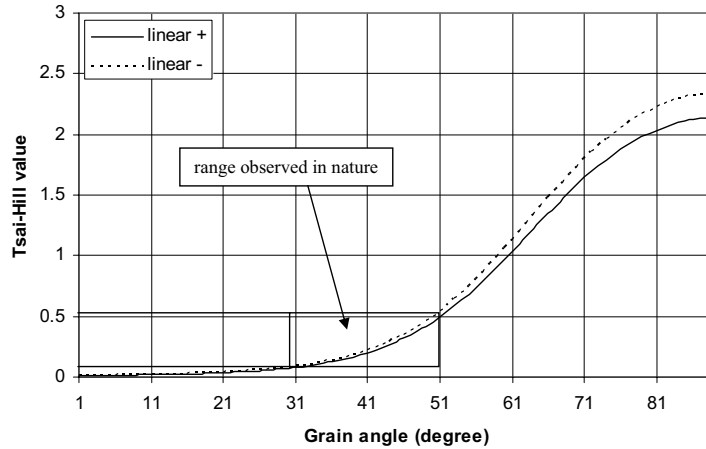


Fig. 3. Failure prediction value for spiralling angle from  $0^\circ$  to  $90^\circ$ : linear analysis.

### 3.3 Transverse displacement

The relationship between the twist of the Ponderosa pine's trunk and its mechanical properties still remains unclear. It is more reasonable to assume that the spiralling is due to the fluid transportation within the structure of the tree. The present analysis shows that excessive spiralling not only reduces the stiffness of the tree but also weakens the strength of the tree. Hence, a limiting point on how much the stiffness can be reduced in order for a tree to stand up straight is observed.

The spiralling is needed to generate enough deflection that does not risk the instability in order to discard excessive snow. The maximum deflection under the assumed geometry and loads shows a large increase between  $30^\circ - 60^\circ$  when comparing the the differences to other intervals of spiralling angle (Fig 5). Most Ponderosa pines observed in Southern Utah shows the spiralling of grain at

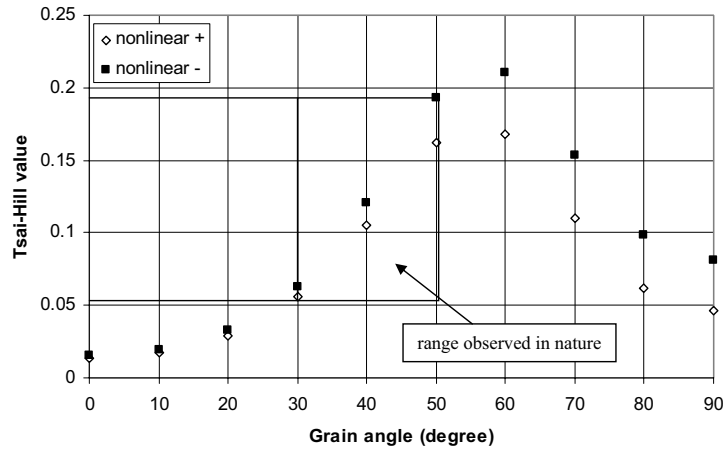


Fig. 4. Failure prediction value for spiralling angle from  $0^\circ$  to  $90^\circ$ : non-linear analysis.

angle between  $30^\circ - 50^\circ$ .

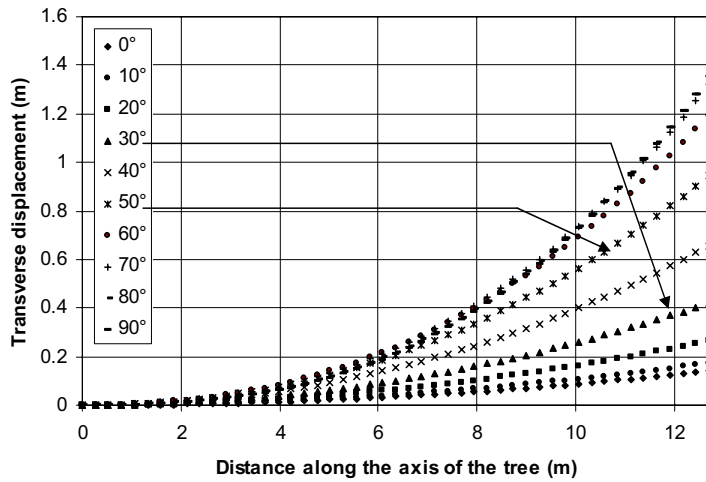


Fig. 5. Transverse displacement along the axis of the tree.

#### 4 Additional factors

- (1) In nature, the grain angle is bigger toward the bottom and reduces toward the top of the tree. When the tree is small, it requires more distribution of fluid to ensure proper growth. Having the fiber spiralling at a bigger angle allows the tree to transport more fluid along its circumference. As the tree grows taller, the angle becomes smaller, which allows the fluid to be transported to the higher portion faster by reducing the coverage area. This could be another reason why the grain angle varies this way.

Details about the fluid transportation are not discussed here since it is beyond the scope of this analysis.

- (2) We did not consider the cracking of the trunk in our analysis which maybe an important factor. Looking at the elastic constants of Ponderosa pine, one finds that  $E_2$  is approximately 5% of  $E_3$ , which is almost as there is a crack. With this in mind, Leonid Slepyan (via private communication) has pointed out that, as the crack wiggles around the tree, it is less prone to fracture than when the crack is vertically straight.
- (3) Due to lack of information and actual data of the average wind load and the load that can uproot the Ponderosa pine, it is not possible to give a solid conclusion regarding relationships between the magnitude of the twist and the elastic properties of trees. In addition, the results presented in this analysis only reflect the Ponderosa pine.

## 5 Conclusion

Our analysis shows that the question of the adaptation of a tree trunk can be viewed as a problem of constrained minimization. The spirals in the grain are developed for the non-mechanical reasons (e.g. transport of the water to branches) and the strength analysis provides a constraint that limits the angle of these spirals. In short, a structure can be more flexible by having the fibers spiral along its circumference. However, depending on the elastic properties of the material, the angle of the spiral can vary.

## References

- [1] Ansys Manual 2000: Element Reference. USA: ANSYS, Inc.
- [2] Ansys Manual 2000: Theory Reference. USA: ANSYS, Inc.
- [3] Bodig, J.; Jayne, B. A. 1982: *Mechanics of Woods and Wood Composites*. New York: Van Nostrand Reinhold
- [4] Cherkaev, A.; Leelavanichkul S. 2004: Why the the grain in tree trunk spirals: a mechanical perspective. In: *Struct Multidisc Optim* **28**. New York: Springer Berlin/Heidelberg, pp. 127-135
- [5] Cherkaev, A.; Slepyan, L. 1999: Waiting Element Structures and Stability Under Extension. In: *J. appl. mech.* **4**. New York: American Society of Mechanical Engineers, pp. 58-82
- [6] The Forest Products Laboratory 1955: *Wood Handbook, No. 19*. Washington, D.C.: U.S. Department of Agriculture, 76

- [7] Gedney, L. 1986: Alaska Science Forum, **Art. 783**
- [8] Kubler, H. 1991: Function of Spiral Grain in Trees. In: *Trees - Structure and Function* **5**. New York: Springer Berlin/Heidelberg, pp. 125-135
- [9] Lekhnitskii, S. G. 1981: Theory of Elasticity of an Anisotropic Body. Moscow: MIR Publishers
- [10] Ting, T.C.T. 1996: Anisotropic Elasticity: Theory and Applications. Oxford: Oxford University Press